OMTN, Volume *28*

Supplemental information

VEGFA-targeting miR-agshRNAs combine efficacy with specificity and safety for retinal gene therapy

Sidsel Alsing, Thomas Koed Doktor, Anne Louise Askou, Emilie Grarup Jensen, Ulvi Ahmadov, Lasse Sommer Kristensen, Brage Storstein Andresen, Lars Aagaard, and Thomas J. Corydon

Supplemental Information

Figure S1

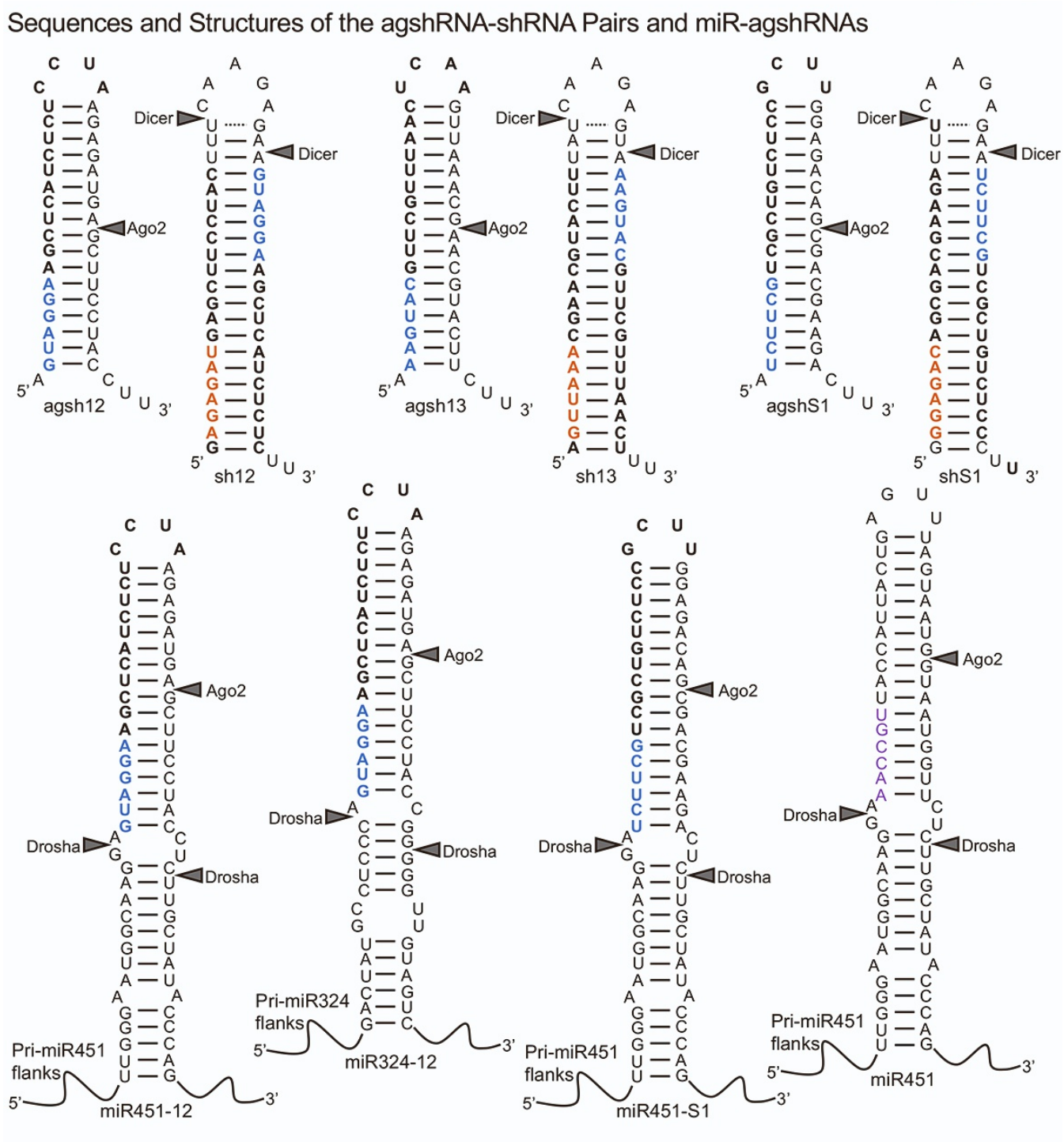

Figure S1. Sequence and Predicted Secondary Structure of the RNAi Effectors. Sequence and predicted secondary structure of three agshRNA-shRNA pairs as well as the miR451-12, miR324-12, miR451-S1, and the endogenous miR451. The pri-miR scaffolds include ~100 nt on both sides of the hairpin. Predicted Ago2, Dicer, and Drosha cleavage sites are indicated. The predicted *VEGFA*/*Vegfa*/S1-targeting agsh12/sh12, agsh13/sh13, and agshS1/shS1 guide strand seed sequences are highlighted in blue, and the predicted sh12, sh13, and shS1 passenger strand seed sequences are highlighted in orange. The guide strand seed sequence of the endogenous miR451 is highlighted in purple. Letters in bold indicate positions with perfect complementarity to the *VEGFA*/*Vegfa* or HIV-S1 sense or AS target (positions 3' of the loop in the agshRNAs with target complementarity are not indicated).

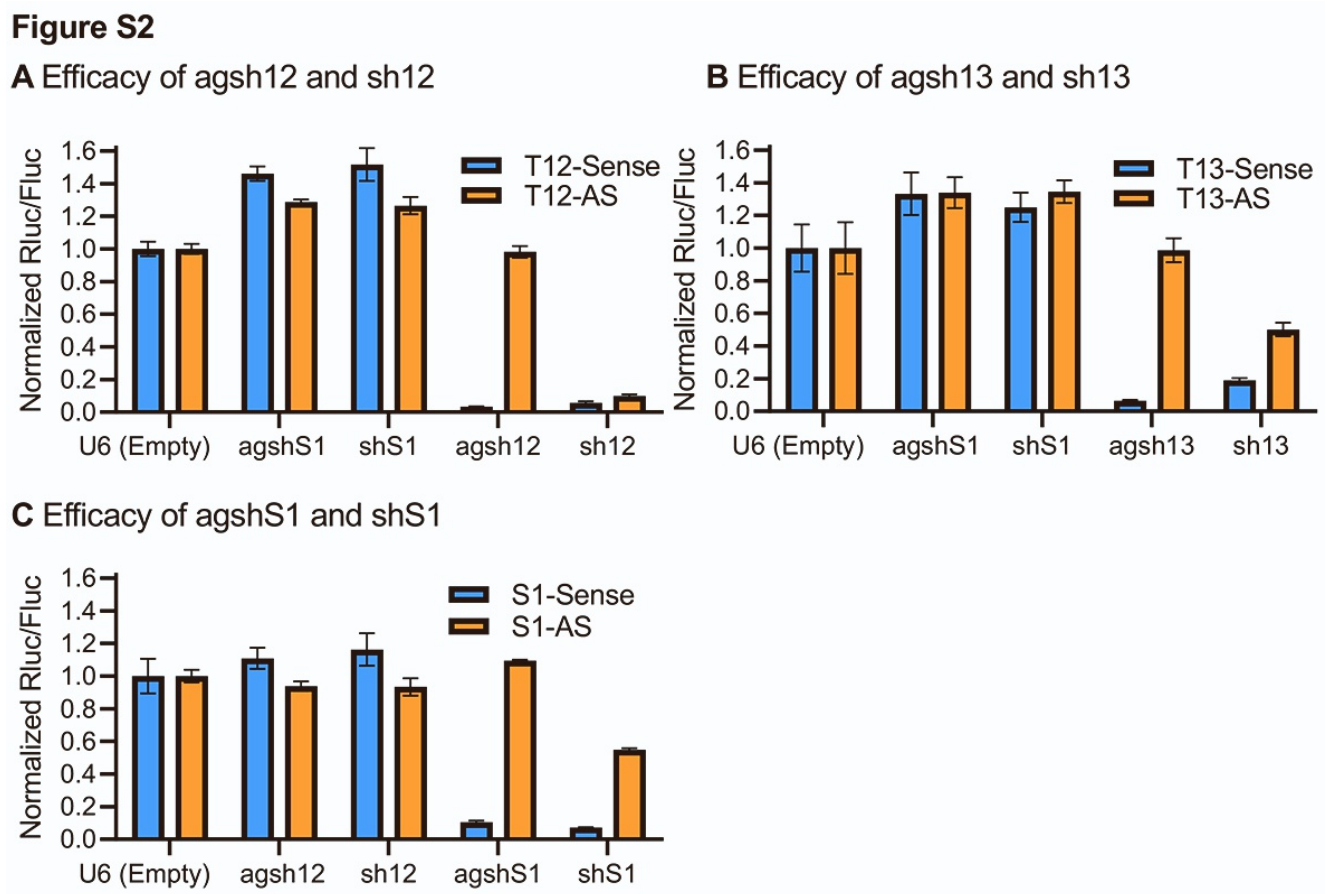

Figure S2. Knockdown Efficacy of the Pol III-driven RNAi Effectors. (A) Knockdown efficacy of the U6-driven agsh12 and sh12 in HEK293 cells measured using the co-transfected dedicated *Vegfa* target region 12 dual luciferase reporters. (B) As in A but with agsh13 and sh13, and the dedicated *Vegfa* target region 13 dual luciferase reporters. (C) As in A and B but with agshS1 and shS1, and the dedicated HIV-1 *tat-rev* transcript site 1 (S1) dual luciferase reporters. The agsh12 and sh12 were included as non-targeting controls. Rluc/Fluc ratio mean of triplicates ± SD normalized to the empty control.

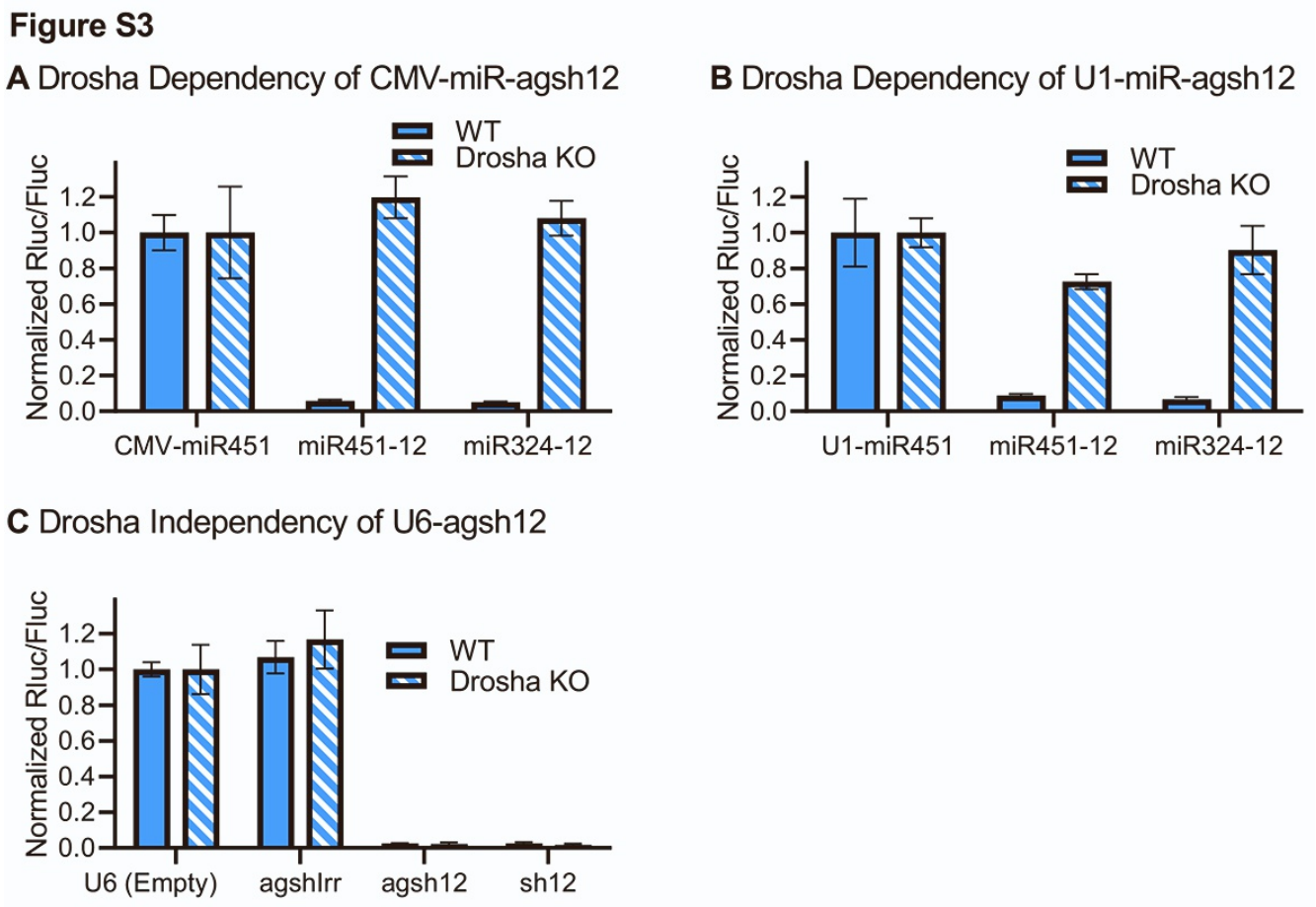

Figure S3. Drosha Dependency of the Pol II-driven RNAi Effectors. (A-B) Drosha dependency was investigated using a Drosha deficient HCT116 cell line.[1] The knockdown efficacy of the CMV or U1 driven miR-agshRNAs in parental HCT116 or Drosha deficient HCT116 was measured using co-transfected dedicated Sense *Vegfa* target region 12 dual luciferase reporter. The non-targeting miR451 was included as a control for normalization. (C) As in A and B but using the U6-driven RNAi effectors. Note that the shRNA in this experiment is the shRNA12.3 which was introduced in our previous publication.[2] and which differs from the sh12 in one nucleotide in the predicted guide and passenger strand. The agshIrr is a non-targeting agshRNA. Rluc/Fluc ratio mean of triplicates ± SD normalized to the endogenous miR451 in A and B, or the Empty U6 vector in C.

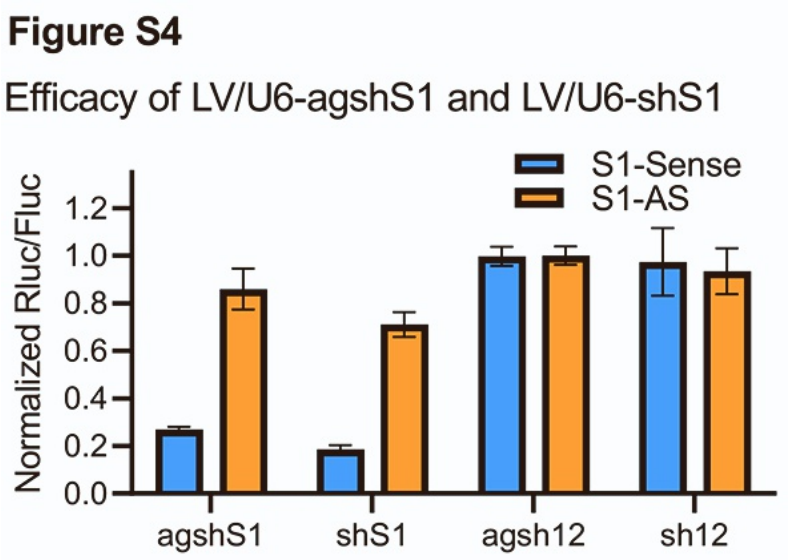

Figure S4. Knockdown Efficacy of the LVs Encoding the Pol III-driven agshS1 and shS1. Knockdown efficacy of LVs encoding the U6-driven agshS1 and shS1. HEK293 cells were transduced with the LVs encoding the RNAi effectors and then transfected with the dedicated HIV-1 *tat-rev* transcript site 1 (S1) dual luciferase reporters. The LVs encoding the U6-driven agsh12 and sh12 were included as controls which do not target the S1 reporters. Rluc/Fluc ratio mean of triplicates ± SD normalized to the agsh12.

Figure S5

A Vector Map of the LV *Vegfa* Minimal Target 12 Reporter

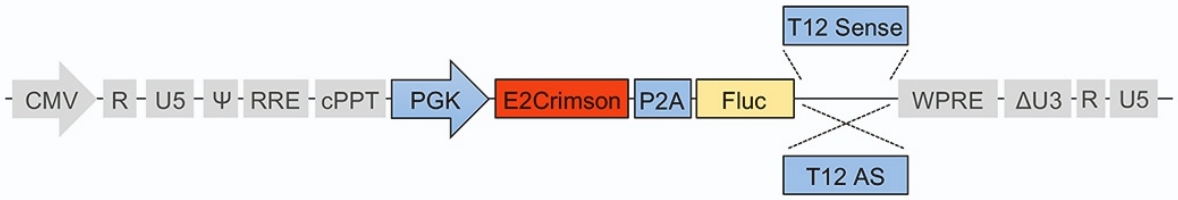

B Evaluation of U1-Driven miR-agshRNA Efficacy Based on E2Crimson Knockdown

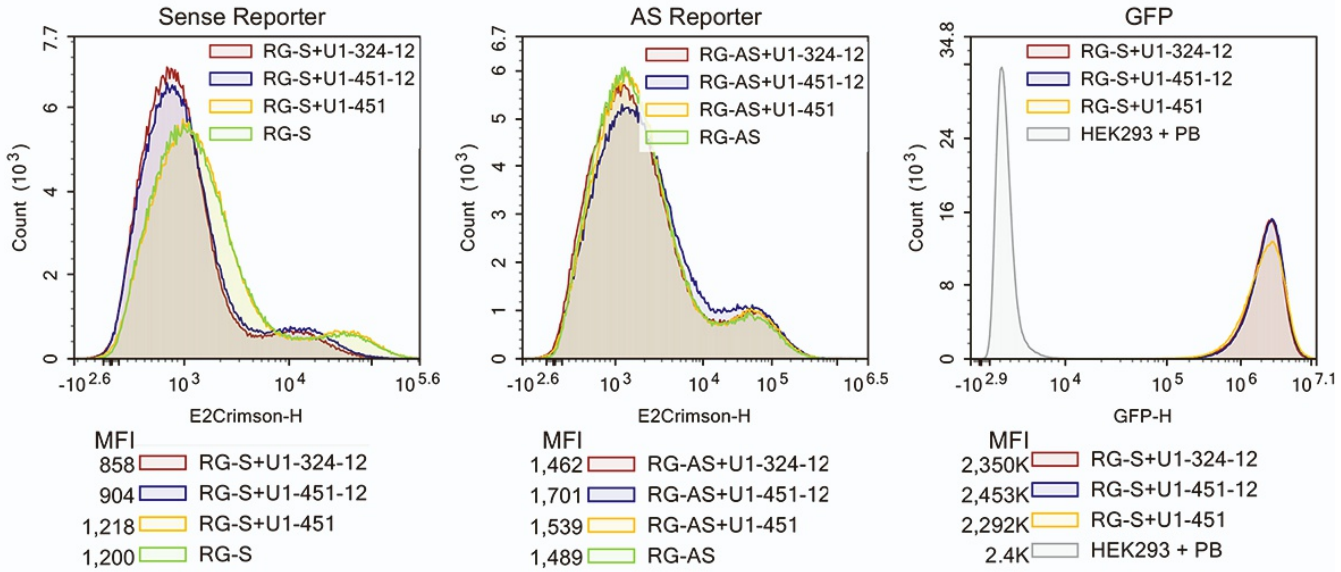

C Evaluation of VMD2-Driven miR-agshRNA Efficacy Based on E2Crimson Knockdown

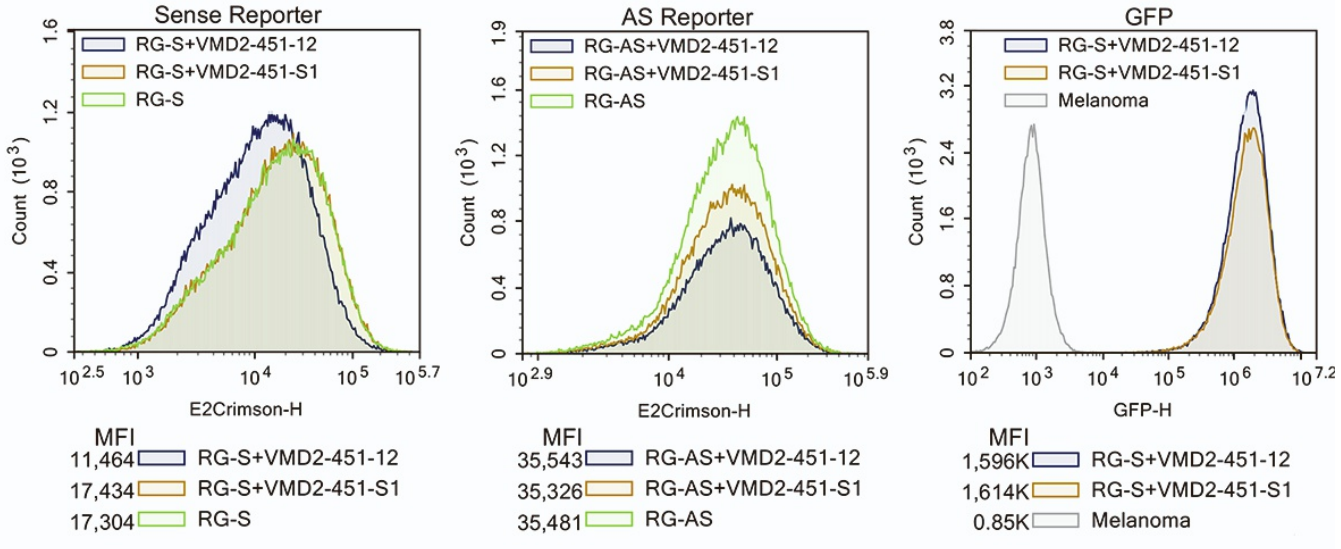

Figure S5. Using the LV *Vegfa* Minimal Target 12 Reporter to Assess Knockdown Efficacy. (A) A schematic vector map of the LV encoding the *Vegfa* minimal target 12 reporter. The PGK promoter drives the expression of the fluorescent protein E2Crimson and Fluc, which are joined by the porcine teschovirus-1 2A (P2A) self-cleaving peptide, and the Fluc is fused to the *Vegfa* minimal target 12 sequence in the sense or the AS direction. (B) The LV-based *Vegfa* minimal target 12 reporter allows evaluation of knockdown of the target 12 based both on a reduction in the expression of the fluorescent protein E2Crimson and on the activity of Fluc (see Figure 4B). Here the expression of E2Crimson and Fluc was evaluated in HEK293 cells transduced with the LV-based *Vegfa* minimal target 12 Sense or AS reporter (RG-S or RG-AS, respectively), and with the LVs encoding the U1-driven RNAi effectors. The EGFP expression from the samples transduced with the LV-based *Vegfa* sense reporter and with the LVs encoding the indicated U1-driven RNAi effectors is also shown, compared to non-transduced polybrene treated HEK293 cells (HEK293 + PB). The median E2Crimson fluorescence intensity (MFI) for each sample is presented below. The flow cytometry analysis and luciferase reporter assay (Figure 4B) were performed 3 days post transduction with the LV encoding the RNAi effector. (C) As in B, except melanoma cells were transduced with the ultracentrifuged LVs encoding the VMD2-driven RNAi effectors (Figure 5A-B). Melanoma cells transduced with the sense or AS reporter were named RG-S or RG-AS, respectively. The EGFP expression was compared to non-transduced melanoma cells.

Supplemental Information

Figure S6

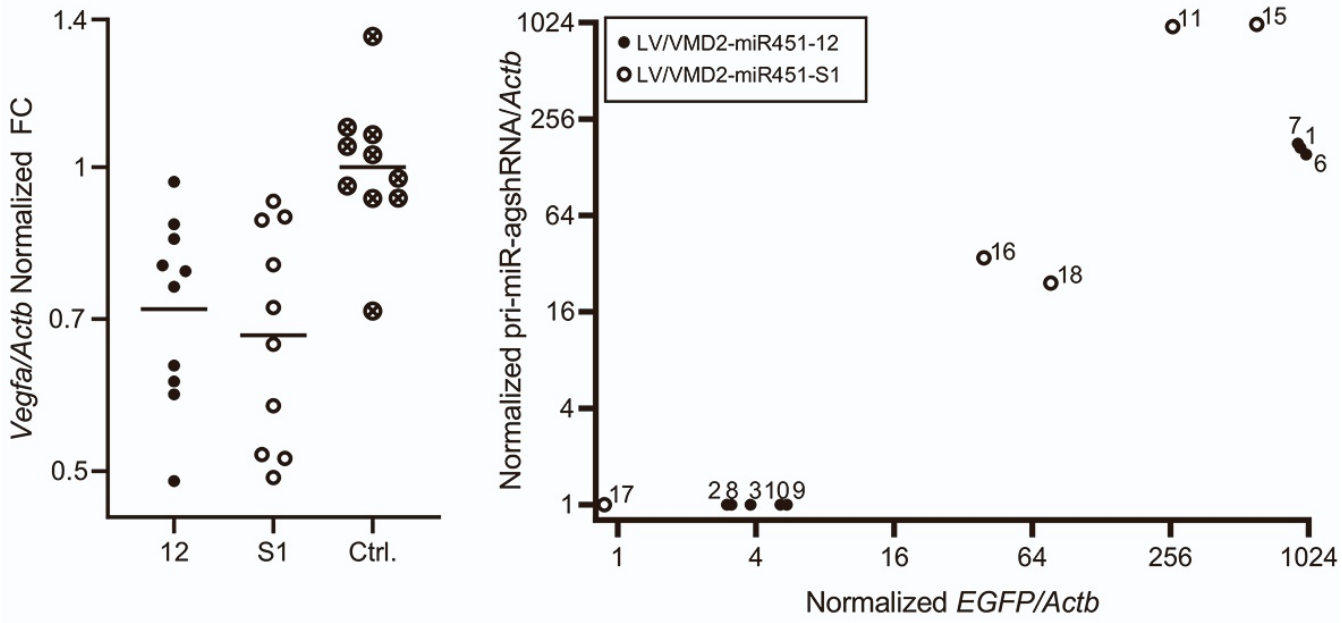

Fundoscopic EGFP Detection in Mice Injected with the LV/VMD2-miR451-12 and LV/VMD2-miR451-S1

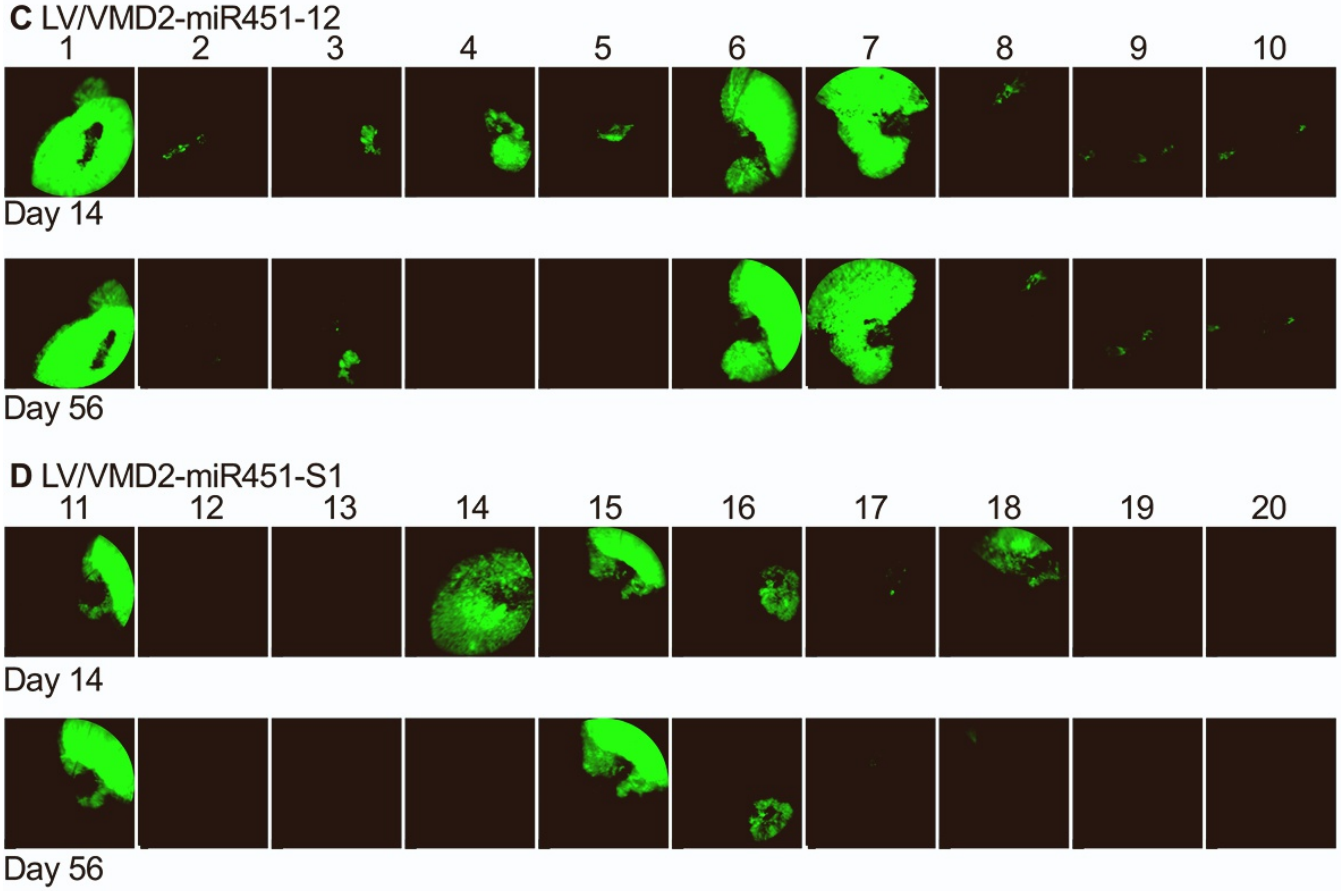

Figure S6. *In Vivo* Expression of *Vegfa*, pri-miR-transcript, and EGFP in Murine Retina (A) The RPE cells from the entire eye cup of mice injected with the LV/VMD2-miR451-12 or LV/VMD2-miR451-S1 were harvested at day 56 p.i. and *Vegfa* mRNA was quantified using RT-qPCR. *Actb*-normalized *Vegfa* fold change (FC) relative to uninjected control eyes with the geometric mean indicated (B) The *Actb*-normalized expression of *EGFP* mRNA and the pri-miR451-agsh transcript was quantified using RT-qPCR. Only data from mice with a detectable level of *EGFP* in RT-qPCR are shown. One sample (mouse 14) was excluded due to a detection of signal in the -RT control. The highest detected expression level was arbitrarily set at 1000 and for mice in which no pri-miR451-agsh transcript was detected, the level was arbitrarily set at 1. The pri-miR451-agshRNA transcripts were detected using primers complementary to 5' and 3' ends of the pri-miR451-agshRNA transcript, not allowing distinction between the miR451-S1 and miR451-12. The transcript was not detected in the RPE cells of the uninjected control eyes in this analysis (data not shown). (C-D) Fundoscopic evaluation of the *in vivo* expression of EGFP in mice injected with the LV/VMD2-miR451-12 or LV/VMD2-miR451-S1 14 days and 56 days p.i.

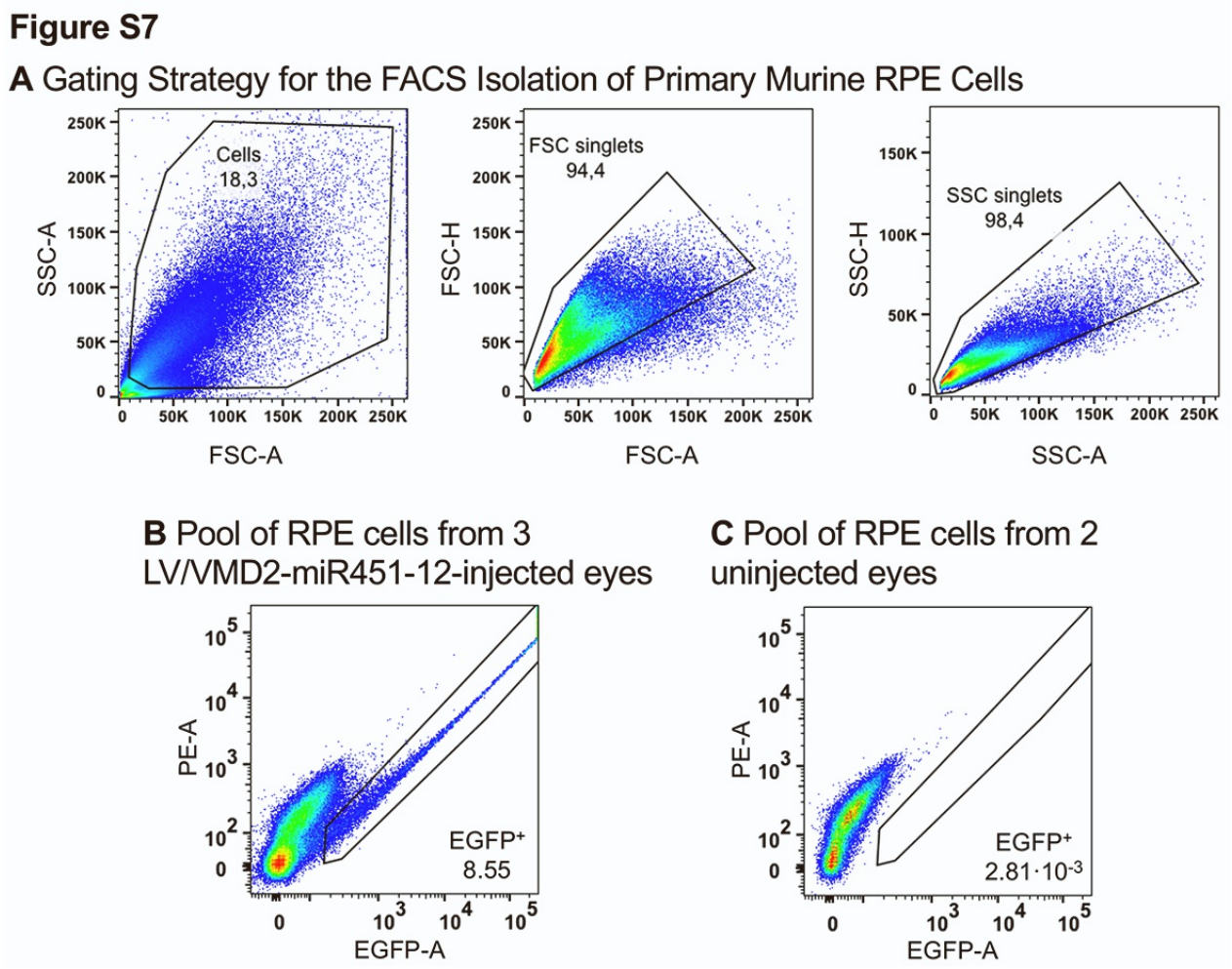

Figure S7. Gating Strategy for the Isolation of EGFP$^+$ RPE Cells. The RPE cells of mice injected with the LV/VMD2-miR451-12 or LV/VMD2-miR451-S1 were harvested at day 14 p.i. RPE cells from 3 injected or 2 contralateral uninjected eyes were pooled prior to FACS based on EGFP expression. (A) Gating of cell population, forward scatter (FSC) singlets, and side scatter (SSC) singlets. A pool of RPE cells purified from 3 eyes injected with the LV/VMD2-miR451-12 is shown as a representative example. (B) EGFP gating of RPE cells from 3 eyes injected with the LV/VMD2-miR451-12. The EGFP$^+$ cells were identified based on fluorescence measured in the EGFP detector (530/30 nm, x-axis) and proportional fluorescence measured in the neighboring PE detector (585/42 nm, y-axis). An equal level of fluorescence in the EGFP and PE detector placing the cells in the diagonal of the plot, was interpreted as autofluorescence and these cells were excluded. The percentage of EGFP$^+$ RPE cells is indicated. (C) Similar gating strategy shown for a pool of 2 uninjected eyes.

Figure S8

LV/VMD2-miR451-S1-PE Injected Eye

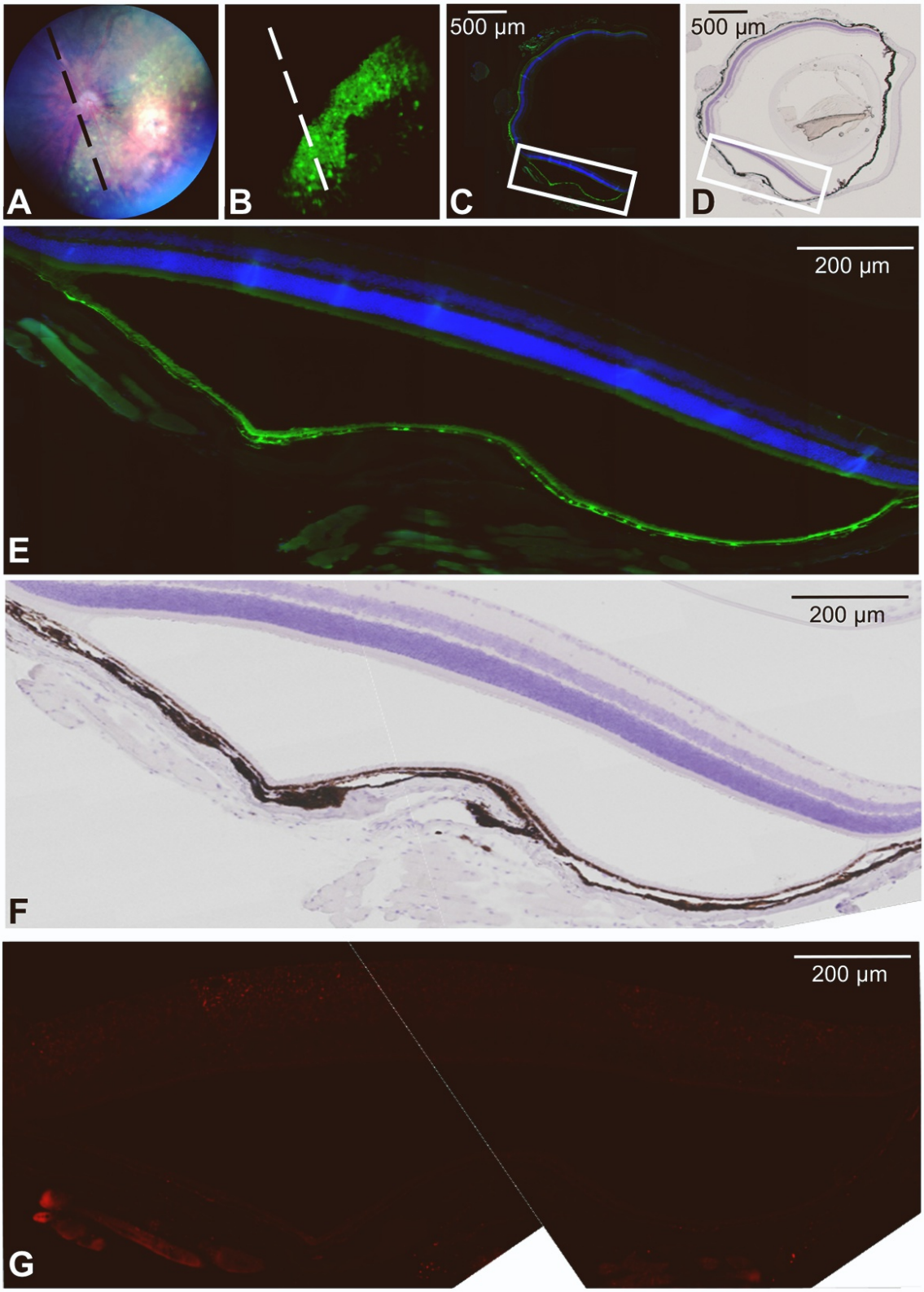

Figure S8. miR451-12 is not Detectable in Control Animals Injected with LV/VMD2-miR-451-S1. (A-B) Brightfield fundoscopy or EGFP detection of the LV/VMD2-miR451-S1 injected eye which was used as a control for the *in situ* detection of miR451-12. The expected position of the cross section used in the analysis is indicated with the dashed line. 57 days p.i. (C) Formalin fixed paraffin embedded cross section of the LV/VMD2-miR451-S1 injected eye, harvested at 57 days p.i. The EGFP signal is shown with DAPI staining. (D) As in C, except here the section adjacent to the section in C is shown, which was used as a control for chromogenic *in situ* detection of the miR451-12. Brightfield image with hematoxylin counterstain. (E) Magnification of the EGFP positive section indicated in C. (F-G) Magnification of the section indicated in D with brightfield or fluorescent detection.

Figure S9

A Downregulated Genes

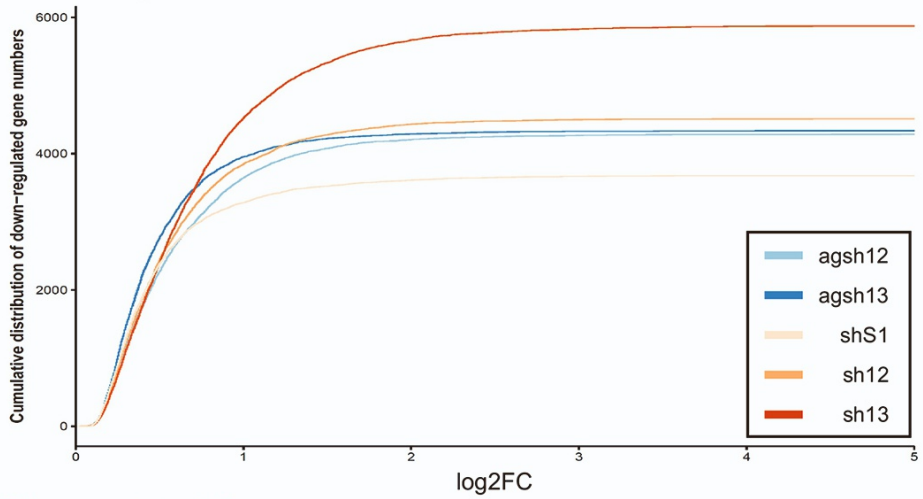

B Upregulated Genes

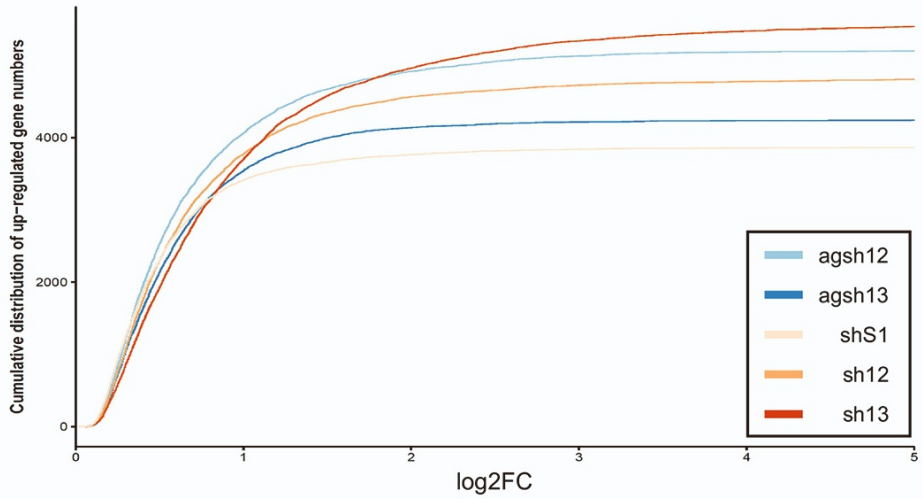

C Heptamer Seed Matches

RNAi Effector	HSMs
12 guide	1899
12 passenger	3686
13 guide	292
13 passenger	1893
S1 guide	548
S1 passenger	3110

D *VEGFA* Expression in ARPE19 Cells Transduced with LV/U6-RNAi Effectors

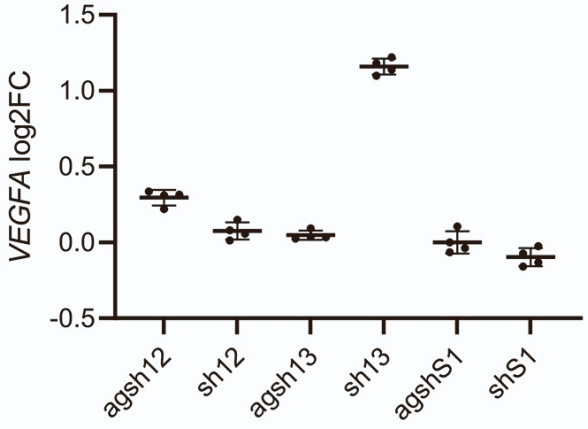

Figure S9. Changes in Gene Expression Levels in ARPE19 Cells Transduced with the LVs Encoding the U6-driven RNAi Effectors. (A) Cumulative count of genes which were downregulated in the ARPE19 cells transduced with the LVs encoding the U6-driven RNAi effectors, compared to the cells transduced with the LV/U6-agshS1. (B) As in A, but with upregulated genes. (C) Table of heptamer seed matches (HSMs) in the 3'UTR of the genes which were expressed in the ARPE19 cells, for each of the RNAi effectors guide and passenger strand. In total 32236 genes were expressed in the ARPE19 cells. (D) ARPE19 cells were transduced with the LVs encoding the Pol III-driven RNAi effectors. The *VEGFA* mRNA log2FC as determined with RNA sequencing is shown relative to the LV/U6-agshS1 transduced cells.

Supplemental Information

Table S1: SOM Hierarchical Clusters GO-BP

Supplied as an Excel file

Table S2: Cloning oligos, sequences, and primers

Name	Sequence
agsh12-A	**GATC**AGTAGGAAGCTCATCTCTCCTAAGAGATGAGCTTCCTACCTTTTT
agsh12-B	**TCGA**AAAAAGGTAGGAAGCTCATCTCTTAGGAGAGATGAGCTTCCTACT
sh12-A	**GATC**GAGAGATGAGCTTCCTACTTTCAAGAGAAGTAGGAAGCTCATCTCTCTTTTT
sh12-B	**TCGA**AAAAAGAGAGATGAGCTTCCTACTTCTCTTGAAAGTAGGAAGCTCATCTCTC
agsh13-A	**GATC**AAAGTACGTTCGTTTAACTCAAGTTAAACGAACGTACTTCTTTTT
agsh13-B	**TCGA**AAAAAGAAGTACGTTCGTTTAACTTGAGTTAAACGAACGTACTTT
sh13-A	**GATC**AGTTAAACGAACGTACTTTATCAAGAGTAAAGTACGTTCGTTTAACTTTTTT
sh13-B	**TCGA**AAAAAAGTTAAACGAACGTACTTTACTCTTGATAAAGTACGTTCGTTTAACT
agshS1-A	**GATC**ATCTTCGTCGCTGTCTCCGCTTGGAGACAGCGACGAAGACTTTTT
agshS1-B	**TCGA**AAAAAGTCTTCGTCGCTGTCTCCAAGCGGAGACAGCGACGAAGAT
shS1-A	**GATC**GGGAGACAGCGACGAAGATTTCAAGAGAATCTTCGTCGCTGTCTCCCTTTTT
shS1-B	**TCGA**AAAAAGGGAGACAGCGACGAAGATTCTCTTGAAATCTTCGTCGCTGTCTCCC
miR451	**CTCGAG**CCAGCTCTGGAGCCTGACAAGGAGGACAGGAGAGATGCTGCAAGCCCAAGAA- GCTCTCTGCTCAGCCTGTCACAACCTACTGACTGCCAGGGCACTTGGGAATGGCAAGGAAACCG TTACCATTACTGAGTTTAGTAATGGTAATGGTTCTCTTGCTATACCCAGAAAACGTGCCAG- GAAGAGAACTCAGGACCCTGAAGCAGACTACTGGAAGGGAGACTCCAGCTCAAACAAGGCAGGG GT**ACCGGT**
miR30	**CTCGAGC**AGAATCGTTGCCTGCACATCTTGGAAACACTTGCTGGGAT- TACTTCTTCAGGTTAACCCAACAGAAGGCTAAAGAAGGTATATTGCTGTTGACAGTGAGCGACT GTAAACATCCTCGACTGGAAGCTGTGAAGCCACAGATGGGCTTTCAGTCGGATGTTT- GCAGCTGCCTACTGCCTCGGACTTCAAGGGGCTACTTTAGGAGCAATTATCTTGTTTACTAAAA CTGAATACCTTGCTATCTCTTTGATACAT**ACCGGT**
miR451-12	**CTCGAG**CCAGCTCTGGAGCCTGACAAGGAGGACAGGAGAGATGCTGCAAGCCCAAGAA- GCTCTCTGCTCAGCCTGTCACAACCTACTGACTGCCAGGGCACTTGGGAATGGCAAGGAGTAGG AAGCTCATCTCTCCTAAGAGATGAGCTTCCTACCTCTTGCTATACCCAGAAAACGTGCCAG- GAAGAGAACTCAGGACCCTGAAGCAGACTACTGGAAGGGAGACTCCAGCTCAAACAAGGCAGGG GT**ACCGGT**
miR451-S1	**CTCGAG**CCAGCTCTGGAGCCTGACAAGGAGGACAGGAGAGATGCTGCAAGCCCAAGAA- GCTCTCTGCTCAGCCTGTCACAACCTACTGACTGCCAGGGCACTTGGGAATGGCAAGGATCTTC GTCGCTGTCTCCGCTTGGAGACAGCGACGAAGACTCTTGCTATACCCAGAAAACGTGCCAG- GAAGAGAACTCAGGACCCTGAAGCAGACTACTGGAAGGGAGACTCCAGCTCAAACAAGGCAGGG GT**ACCGGT**
miR324-12	**CTCGAG**TTCTTAAAAGGGGTGGATGTAAGGGATGAGGTAGAATTAACTTCTGGTACTGCTGG- CAGGCACCTGAGCAGAACATCATTGCTGTCTCTCTTCGCAGAAGCTGAGCTGACTATGCCTCCC AGTAGGAAGCTCATCTCTCCTAAGAGATGAGCTTCCTACCGGGGGTTGTAG- TCTGACCCGACTGGGAAGAAAGCCCCAGGGCTCCAGGGAGAGGGGCTTGGGAGGCCCTCACCTC AGTTACATACTGCAGCATAACCATCCGTGCCAGCTTCTCCTGGATCAGCCCAAAGTT- GTGAA**ACCGGT**

Supplemental Information

SalI-miR451-fwd	AGACC**GTCGAC**CTCGAGCCAGCTCTGGAGC
BclI-miR451-rev	GAGGC**TGATCA**GCGGGTTTAAACG
S1-Sense-A	**TCGA**AAGCGGAGACAGCGACGAAGAGCT
S1-Sense-B	**GGCC**AGCTCTTCGTCGCTGTCTCCGCTT
S1-AS-A	**TCGA**AGCTCTTCGTCGCTGTCTCCGCTT
S1-AS-B	**GGCC**AAGCGGAGACAGCGACGAAGAGCT
min-*Vegfa*-T12 – Sense-A	**CGCG**TACATAGGAGAGATGAGCTTCCTACAGCACAC
min-*Vegfa*-T12 – Sense-B	**TCGA**GTGTGCTGTAGGAAGCTCATCTCTCCTATGTA
min-*Vegfa*-T12 – AS-A	**CGCG**TTGTGCTGTAGGAAGCTCATCTCTCCTATGTC
min-*Vegfa*-T12 – AS-B	**TCGA**GACATAGGAGAGATGAGCTTCCTACAGCACAA
pCCL-MCS-5'PGK Fwd	GAGAGA**ATCGAT**TACGAGCGTACGACTAGCCTCGACGATGGTCGAGTAC
pCCL-MCS-3'PGK Rev	GAGAGA**CTCGAG**AGCGCACGCGTTATATCCCGGGACACAGGGCCCGAGAGTCTA-GACTCTCGTCGACCTATAGGATCCCGCTAGAGGTCGAAAGGC
BamHI *EGFP* Fwd	ATATA**GGATCC**GCCACCATGGTGAGCAAGGGCGAGG
XbaI *EGFP* Rev	TGTGT**TCTAGA**TTACTTGTACAGCTCGTCCATGC

Restriction site compatible overhangs are indicated in bold.

Supplemental Information

Table S3: qPCR Primers

Name	Sequence	Length of amplicon
ALB Fwd	GCTGTCATCTCTTGTGGGCTGT	139
ALB Rev	ACTCATGGGAGCTGCTGGTTC	
ALB Probe	CCTGTCATGCCCACACAAATCTCTCC	
WPRE Fwd	GGCACTGACAATTCCGTGGT	108
WPRE Rev	AGGGACGTAGCAGAAGGACG	
WPRE Probe	ACGTCCTTTCCATGGCTGCTCGC	
VEGFA Fwd	ACAACAAATGTGAATGCAGACCA	165
VEGFA Rev	TTAACTCAAGCTGCCTCGCC	
PPIA Fwd[b]	AGACAAGGTCCCAAAGAC	118
PPIA Rev[b]	ACCACCCTGACACATAAA	
HPRT1 Fwd[b]	GACCAGTCAACAGGGGACAT	132
HPRT1 Rev[b]	CCTGACCAAGGAAAGCAAAG	
GAPDH Fwd[b]	GACAGTCAGCCGCATCTTCT	127
GADH Rev[b]	TTAAAAGCAGCCCTGGTGAC	
Vegfa Fwd[a]	CAGGCTGCTGTAACGATGAA	207
Vegfa Rev[a]	AATGCTTTCTCCGCTCTGAA	
Hprt Fwd[a]	CTTTGCTGACCTGCTGGATT	179
Hprt Rev[a]	CAACAATCAAGACATTCTTTCCA	
Actb Fwd	CTAAGGCCAACCGTGAAAAG	104
Actb Rev	ACCAGAGGCATACAGGGACA	
Rn18s Fwd	CTCAACACGGGAAACCTCAC	110
Rn18s Rev	CGCTCCACCAACTAAGAACG	
SalI-miR451-fwd[c]	AGACC**GTCGAC**CTCGAGCCAGCTCTGGAGC	295
BclI-miR451-rev[c]	GAGGC**TGATCA**GCGGGTTTAAACG	
EGFP Fwd	GGTGAACTTCAAGATCCGCC	229
EGFP Rev	CTTGTACAGCTCGTCCATGC	
Actb 2 Fwd	CACTGTCGAGTCGCGTCC	89
Actb 2 Rev	TCATCCATGGCGAACTGGTG	

[a]Previously validated.[3]

[b]Previously validated.[4]

[c]Primers also used for cloning.

1. Kim, Y.-K., Kim, B., and Kim, V.N. (2016). Re-evaluation of the roles of DROSHA, Exportin 5, and DICER in microRNA biogenesis. Proceedings of the National Academy of Sciences of the United States of America *113*, E1881-E1889. 10.1073/pnas.1602532113.
2. Kaadt, E., Alsing, S., Cecchi, C.R., Damgaard, C.K., Corydon, T.J., and Aagaard, L. (2019). Efficient Knockdown and Lack of Passenger Strand Activity by Dicer-Independent shRNAs Expressed from Pol II-Driven MicroRNA Scaffolds. Molecular therapy. Nucleic acids *14*, 318-328. 10.1016/j.omtn.2018.11.013.

3. Askou, A.L., Alsing, S., Benckendorff, J.N.E., Holmgaard, A., Mikkelsen, J.G., Aagaard, L., Bek, T., and Corydon, T.J. (2019). Suppression of Choroidal Neovascularization by AAV-Based Dual-Acting Antiangiogenic Gene Therapy. Molecular therapy. Nucleic acids *16*, 38-50. 10.1016/j.omtn.2019.01.012.
4. Liu, X., Xie, J., Liu, Z., Gong, Q., Tian, R., and Su, G. (2016). Identification and validation of reference genes for quantitative RT-PCR analysis of retinal pigment epithelium cells under hypoxia and/or hyperglycemia. Gene *580*, 41-46. 10.1016/j.gene.2016.01.001.